

## A New Analytical Model for High Heat Flux in Pool Boiling

<sup>1</sup>Guoping Jiang, <sup>2</sup>Boqi Xiao and <sup>1</sup>Jichao Liu

<sup>1</sup>Earthquake Engineering Research Test Center, Guangzhou University,  
Guangzhou 510405, China

<sup>2</sup>Department of Physics and Electromechanical Engineering, Sanming University,  
Sanming 365004, China

**Abstract:** In this study, first the empirical correlations and primary models of Critical Heat Flux (CHF) are introduced, then a new fractal model for critical heat flux is proposed. Algebraic expressions for the fractal dimension of nucleation sites are derived based on the fractal distribution of nucleation sites, which are shown to be a strong function of wall superheat. The new fractal model for critical heat flux is found to be a function of wall superheat. The contact angle of the fluid and the physical properties of the fluid and empirical constant have an important effect on critical heat flux. It turns out that the present model well explains the mechanism on how parameter such as surface wettability influences CHF. The present model shows the surface wettability plays no significant role. The expressions of active nucleation site are applied to CHF which are predicted in the proposed model quantitatively. The predicted critical heat flux from a boiling surface based on the proposed fractal model is compared with existing experimental data. An excellent agreement between the new model predictions and experimental data is found. The validity of the new fractal model is thus verified.

**Keywords:** Critical heat flux, fractal model, heat transfer rates, pool boiling, thermodynamics

### INTRODUCTION

Pool boiling is associated with a change in phase from liquid to vapor at a solid-liquid interface, which is characterized by the formation of vapor bubbles that nucleate, grow and subsequently detach from the locations of nucleation sites, that occurs when the surface temperature is at the corresponding liquid pressure. In pool boiling the Critical Heat Flux (CHF) is widely applied in engineering and technology. The strong interest is due to practical applications since it is desirable to design an efficient heat exchanger or boiler to operate at as high heat flux as possible with optimum heat transfer rates without risk of physical burnout. Over the past decades the mechanisms of CHF has been widely investigated. In the literature there are a lot of empirical correlations and models for CHF, with each applicable to a restricted range of experimental conditions (Dhir and Liaw, 1989; Kocamustafaogullari and Ishii, 1983; Del Valle and Kenning, 1985; Lorenz and Mikic, 1974). From a mechanistic viewpoint, the influences of some parameters such as heater geometry, roughness surfaces and contact angle etc. have extensively been discussed, but an overall mechanistic description is still unavailable. In addition, each model has its disadvantages because of the limitations of experiment conditions. So, searching a

comprehensive theory and unified model becomes a challenging task. From the above brief review it is seen that a mechanistic model for CHF has not yet been developed. The modeling should be such that the empirical relations used represent the physical process of pool boiling phenomena at CHF.

In this study, we attempt to develop a new analytical Model for high Heat Flux in Pool boiling based on the fractal characteristics of sizes of active cavities on heated surfaces.

**Regime I:** Natural convection regime. Heat is transferred by free convection. Wall superheat does not exceed 5°C.

Regime II and Regime III is called nucleate boiling regime. Wall superheat is in the range of 5°C-30°C in the two regimes.

**Regime II:** The region of isolated bubbles. In this range, bubbles rise from isolated nucleation sites. As  $q$  and  $\Delta T$  increase, more and more sites are activated.

**Regime III:** The region of slugs and column. When the active sites become very numerous, the bubbles start to merge into one another,

and an entirely different kind of vapor escape path comes into play. Vapor formed at the surface merges immediately into jets which feed into large overhead bubbles of “slug” of vapor. The major is regime III in this study.

**Regime IV:** Transitional boiling regime.

**Regime V:** Film boiling.

CHF, point D, is called the burnout point. It is the condition at which the increased heat flux produced by a rise in  $\Delta T$  is offset by the increased resistance of the vapor blanket around the heater. Then the temperature difference is low while the heat flux is very high. Heat transfer coefficients in this range are enormous. Clearly, it is very desirable to be able to operate heat exchange equipment at the upper end of the region III. However, it is very dangerous to run equipment near CHF in systems in which  $q$  is given independently of  $\Delta T$ . If  $q$  is raised beyond the upper limit of the nucleate boiling regime, such a system will suffer a sudden and damaging increase of temperature.

## METHODOLOGY

### Empirical correlations and primary models of CHF:

The mechanism of CHF is one of the most controversial subjects for heat transfer in pool boiling. Many of the published CHF models have been based on postulated mechanism at the present time. And various correlations and models of CHF are derived. The representative correlations and models are introduced in the following section.

**Empirical correlations:** Addoms (1948) proposed that buoyancy lift and thermal diffusivity of fluid are the controlling parameters of CHF. He applied dimensional analysis method to obtain the following correlation:

$$q_{CHF} = ch_{fg}\rho_g \left( \frac{gk_f}{\rho_f c_{pf}} \right)^{1/3} \left( \frac{\rho_f - \rho_g}{\rho_g} \right)^{1/2} \quad (1)$$

Kutateladze (1951) recognized that burnout resembled the flooding of a distillation column. At any level in a distillation column, alcohol-rich vapor (for example) rises while water-rich liquid flows downward in counterflow. If the process is driven too far, the flows become Helmholtz-unstable and the process collapses. The liquid then cannot move downward and the column is said to “flood”. Kutateladze did the dimensional analysis of CHF based on the flooding mechanism and obtained the following relationship:

$$c = \frac{q_{CHF}}{\rho_g^{1/2} h_{fg} \left[ g \sigma (\rho_f - \rho_g) \right]^{1/4}} \quad (2)$$

He then suggested that  $c$  was equal to 0.131 on the basis data from configurations other than infinite fiat plates. The experimental data indicated that  $c$  was in the range of  $c = 0.13-0.16$  for different surfaces of various liquids on wire and plate. Zuber *et al.* (1962) pointed that the formula of CHF is derived which is the same as Eq. (2) from one of the following mechanisms:

- The accumulation and coalescences of bubbles on wall and interference of vapour stems each other.
- Vapour phase of upward movement results in instability and split of liquid.
- Vapour phase of upward movement results in suspension or split of the micro liquid drop.

### Primary models of CHF:

- **Bubble interference model:** The model assumed that bubbles were impeded to removed from the heating surface when heat flux reached CHF. This case was described by motion speed of bubbles. With analysis of energy balance, latent heat flux of evaporation is entrapped by bubbles which is CHF when motion speed of bubbles reaches a critical value. CHF is expressed as:

$$q_{CHF} = h_{fg}\rho_g \left( \frac{\pi}{6} D_b^3 n_0 f \right)_{CHF} \quad (3)$$

where,  $\left( \frac{\pi}{6} D_b^3 n_0 f \right)_{CHF}$  is called motion speed of bubbles at CHF,  $n_0$  is wall density of bubbles,  $D_b$  is departure diameter which is associated with contact angles  $\phi$ . The  $c$  is obtain by substituting Eq. (3) into (2). Various researchers applied different expressions of parameters. This case results in the difference for calculation. That  $c$  is in the range of 0.17-0.24 if contact angles  $\phi$  in the range of 46°-60°. Particularly, bubble interference model has disadvantage for the accumulation and coalescences of much bubbles. Bubble interference model was based on analysis of isolated bubble. However, the accumulation and coalescences of bubbles are not neglected at CHF.

- **Hydrodynamic instability model:** The primary viewpoint of the model was that flow instability of boundary of two phase flow between vapour and liquid near wall was the principal cause for conversion from nucleate boiling to film boiling. The rounded wave theory of heat flux was proposed by Zuber and Westwater (1961) as:

$$0.15 > \frac{q_{CHF}}{h_{fg}\rho_g} \left( \frac{\rho_g^2}{\sigma g (\rho_f - \rho_g)} \right)^{1/4} > 0.12 \quad (4)$$

Kutateladze's Eq. (2) was proved by Zuber, which is Zuber's theoretical significance. It is needless that data is derived from isolated bubble region. But CHF is determined by fluid mechanism strictly, which is a controversial problem and independent on state of surface. The hydrodynamic instability model is based on two dimensional theory of fluid mechanism. However, practical situation is that the model is based on three dimensional theory of fluid mechanism, which is simplified which involves the difference of parameter mostly.

- **Liquid film dryout model:** The model is derived according to experimental observation and theoretical analysis. Quite a few mushroom vapor bubbles are formed on wall when heat flux is higher at the last time of nucleate boiling. The liquid film of given thickness exists between bottom of big bubbles and wall. CHF is expressed as

$$q_{CHF} = \frac{t_{ev}}{t_g} q_n \tag{5}$$

where,  $t_{ev}$  is average time of liquid film dryout,  $t_g$  is growth time of big bubble,  $q_n$  is the heat flux of liquid film for boiling. But the result is obtained which is lower from Eq. (5) than that is from actual measurement.

**Fractal analysis of nucleation:**

**Sites on a boiling surface:** The research on the effects of the roughness of heating surface in pool boiling has made great advances over the last several decades. Mikic and Rohsenow (1969) and Lorenz (1974) proposed the following mathematical model:

$$N = C_0 \left( \frac{r_l}{r_{min}} \right)^m \tag{6}$$

where,  $r_l$  is the mouth radius of the cavity,  $C_0$  a dimensional constant ( $1/area$ ),  $m$  a constant characterizing a boiling surface. (Majumdar and Tien, 1987) describe the rough surface with the help of fractal geometry and obtained the following equation about the cavity distribution on the surface:

$$N(R > r) = \left( \frac{r_{max}}{r} \right)^{d_f} \text{ and } r_{min} < r < r_{max} \tag{7}$$

where,  $N$  is the number of the cavities on the rough surface,  $d_f$  is the fractal dimension of cavity. The minimum active cavity radius  $r_{min}$  and the maximum active cavity radius  $r_{max}$  could be predicted by Hsu (1962) model for active cavity radius, i.e.,

$$r_{min} = \frac{\delta}{C_1} \left[ 1 - \frac{\theta_s}{\theta_w} - \sqrt{\left( 1 - \frac{\theta_s}{\theta_w} \right)^2 - \frac{4\zeta C_3}{\delta \theta_w}} \right] \tag{8a}$$

$$r_{max} = \frac{\delta}{C_1} \left[ 1 - \frac{\theta_s}{\theta_w} + \sqrt{\left( 1 - \frac{\theta_s}{\theta_w} \right)^2 - \frac{4\zeta C_3}{\delta \theta_w}} \right] \tag{8b}$$

where,  $\zeta = \frac{2\sigma T_s}{\rho_s h_{fg}}$ ,  $C_1 = \frac{(1 + \cos \phi)}{\sin \phi}$  and  $C_3 = 1 + \cos \phi$  with  $\phi$  being the contact angel of the fluid and the heater material.  $\delta$  is the thermal boundary layer thickness which can be expressed:

$$\delta = \frac{k_f}{h_{nc}} \tag{9a}$$

where,  $\delta$  is derived 0.1 mm order for water. The correlation is obtained between  $\delta$  and  $\Delta T$  from Eq. (9a) when the horizontal plate is immersed in water under definitive atmospheric pressure as:

$$\delta = 1.38 \times 10^{-3} \sqrt[3]{\Delta T} \tag{9b}$$

Hsu pointed out that a cavity can be active in the range of  $r_{min} < r < r_{max}$ . A cavity can be ineffective at low wall temperature (or low heat flux). The wall temperature and heat flux are very high at heat flux approaching CHF. So the scales of active cavity are described by Hsu, which are very appropriate.

In this study, we consider the active cavities formed on the heated surface are analogous to pores in porous media. Based on this concept, we can take advantages of recent developments on fractal theory of porous media. In particular, (Yu and Cheng, 2002a) found that the cumulative number of pores in porous media with the diameter larger than and equal to a particular value,  $D_s$ , obeys the following fractal scaling law (Mandelbrot, 1982; Feder, 1988; Majumdar and Bhushan, 1990):

$$N(D_L \geq D_s) = \left( \frac{D_{s,max}}{D_s} \right)^{d_f} \text{ and } D_{s,min} \leq D_s \leq D_{s,max} \tag{10a}$$

where,  $D_{s,max}$  is the maximum diameter of pores in porous media,  $D_s$  is the diameter of a pore and  $d_f$  is the area fractal dimension. If active cavities formed on the heated surface are considered as pores in porous media, the cumulative number of active cavities with diameter greater than and equal to  $D_c$  is also described by Eq. (10b) with  $N$  and  $D_s$  replaced by  $N_a$  and  $D_c$ , respectively, i.e.,

$$N_a(D_L \geq D_c) = \left( \frac{D_{c,max}}{D_c} \right)^{d_f} \text{ and } D_{c,min} \leq D_c \leq D_{c,max} \tag{10b}$$

where,  $D_{c,max} = 2r_{max}$ ,  $D_{c,min} = 2r_{min}$ . In fact, (Majumdar, 1992) discussed such a possibility and pointed

out that the active cavities on the heated surface should also follow the power law by Eq. (10a). The total number of nucleation sites from the minimum active cavity to the maximum active cavity can be obtained from Eq. (10b) as:

$$N_{a,tot} = N_a (D_L \geq D_{c,min}) = \left( \frac{D_{c,max}}{D_{c,min}} \right) d_f \quad (11)$$

In nucleate pool boiling, the fractal dimension  $d_f$  of nucleation sites is given by Yu as:

$$d_f = \frac{\ln \left[ \frac{1}{2} \left( \frac{\bar{D}_{c,max}}{D_{c,min}} \right)^2 \right]}{\ln \frac{D_{c,max}}{D_{c,min}}} \quad (12)$$

where  $\bar{D}_{c,max}$  is the averaged value over all the maximum active cavities which was derived by (Yu and Cheng, 2002b) as:

$$\begin{aligned} \bar{D}_{c,max} &= \frac{1}{(T_w - T_s)} \int_{T_s}^{T_w} D_{c,max}(T_w) dT_w \\ &= \frac{1}{\Delta T} \sum_{j=1}^m D_{c,max}(T_{w_j}) \delta T_w = \frac{1}{m} \sum_{j=1}^m D_{c,max}(T_{w_j}) \end{aligned} \quad (13)$$

where,  $m = \Delta T / \delta T_w$  and we have assumed that  $\delta T_w$  is a constant. In the above equation,  $T_{w_j} = T_s + j(\delta T_w)$  with  $j = 1, 2, \dots, m$ , For example, if we choose  $\delta T_w = 0.2^\circ\text{C}$  then  $m = 5$  for  $\Delta T = 1^\circ\text{C}$  and  $m = 50$  for  $\Delta T = 10^\circ\text{C}$ .

Figure 1 is a plot of the fractal dimension versus wall superheat for  $\phi = 14^\circ$ ,  $\phi = 38^\circ$  and  $\phi = 69^\circ$ , respectively.

According to the fractal geometry theory, the fractal dimension  $d_f$  should be in the range of  $1 < d_f < 2$ , in a two dimensional space. Figure 1 shown that the fractal dimension  $d_f$  is in the range of  $1 < d_f < 2$  when wall superheat are given in the range of  $10^\circ \leq \Delta T \leq 100^\circ$  for contact angles  $\phi = 14^\circ$ ,  $\phi = 38^\circ$  and  $\phi = 69^\circ$ . This means that the number of active nucleate sites versus sizes is fractal if they are in the wall superheat as specified above. This shows that the contact angel affects the initiation of nucleate sites exhibiting the fractal behaviors. It is shown that a high value of the contact angel results in a higher value of  $d_f$ . For example, at  $\Delta T = 10^\circ\text{C}$ , Eq. (12) gives  $d_f = 1.853$  for  $\phi = 14^\circ$ ,  $d_f = 1.855$  for  $\phi = 38^\circ$  and  $d_f = 1.863$  for  $\phi = 69^\circ$ . Figure 1 shown that the fractal dimension increase from  $d_f = 1.853$  and approaches a value of  $d_f = 2$  at  $\phi = 14$  as wall superheat is increases from  $\Delta T = 10^\circ\text{C}$  to infinity. However, the wall superheat in reality would not reach infinity and can also reach a finite value during nucleate pool boiling experiments.

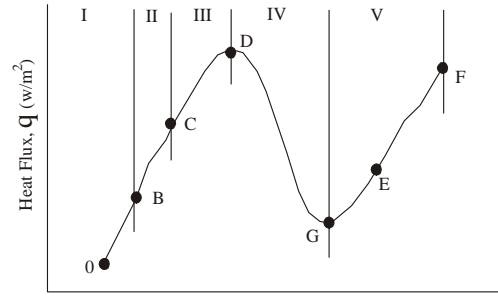


Fig. 1: Wall superheat,  $\Delta T(T_w - T_s)^\circ\text{C}$

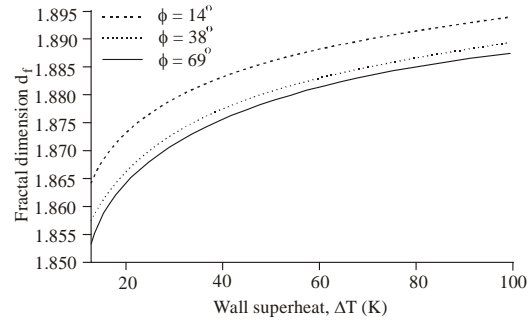


Fig. 2: Fractal dimension versus wall superheat for  $\phi = 14^\circ$ ,  $\phi = 38^\circ$

**The calculation of CHF in pool boiling:** Gaertner (1963) discovered that the bubble sites on a boiling surface are randomly distributed and can be represented by Poisson distribution. Furthermore, (Sultan and Judd, 1978; Del Valle and Kenning, 1985; Wang and Dhir, 1993) reported that the distribution of local cavity population densities is described by the Poisson distribution. Kang *et al.* (1994) proposed a probability model using Poisson distribution to predict the transition points on the boiling curve. So the Poisson distribution can predict point D in Fig. 2. Unfortunately, they did not predict the curve quantitatively. Ha (1998) described active nucleate sites by Poisson distribution. The overall heat flux is expressed by the following equation:

$$q_{tot} = q_b N_a [1 - P(n \geq n_c)] \quad (14)$$

where,

$$P(n \geq n_c) = 1 - \sum_{n=0}^{n_c-1} p(n) \quad (15)$$

$$P(n) = \frac{e^{-N_a A} (N_a A)^n}{n!} \quad (16)$$

where,  $q_b$  is heat transferred by single bubble site assuming each bubble site has uniform heat duty.  $A$  is cell area in Ha's model.  $n_c$  is a critical site number to form the dry spot under a bubble and determined by 5 in Ref. In

Table 1: Contribution of three mechanisms to nucleate boiling heat transfer of water at  $\phi = 90^\circ$

$\Delta T(^{\circ}C)$	$q_b$	$q_{me}$	$q_{nc}$
10	5.83E+04	1.29E+04	7.05E+03
11	9.00E+04	1.56E+04	7.22E+03
12	1.33E+05	1.85E+04	7.33E+03
13	1.90E+05	2.17E+04	7.38E+03
14	2.63E+05	2.51E+04	7.37E+03
15	3.55E+05	2.87E+04	7.30E+03
16	4.70E+05	3.25E+04	7.18E+03
17	6.09E+05	3.64E+04	7.01E+03
18	7.77E+05	4.06E+04	6.78E+03
19	9.76E+05	4.50E+04	6.51E+03
20	1.21E+06	4.95E+04	6.19E+03

this study, we describe the active nucleate site  $N_a$  by fractal theory quantitatively.  $N_a$  can be obtained from Eq. (11).

It is generally recognized that there are three main mechanisms contributing to nucleate boiling heat transfer: the bubble generation and departure from nucleation sites on the superheated surface ( $q_b$ ), natural convection on inactive nucleation areas of the heated surface ( $q_{nc}$ ) and micro-layer evaporation underneath the bubbles ( $q_{me}$ ). For high heat flux up to CHF, it is generally known that the heat flux fractions due to natural convection and due to evaporating microlayer are much smaller than that duo to nucleate boiling. So Eq. (14) can predict CHF exactly. The data is derived from Yu in Table 1, which proved the above conclusion. Table 1 shown that an increase of  $\Delta T$  leads to an increase  $q_b$ . But an increase of  $\Delta T$  leads to a decrease  $q_{nc}$  and  $q_{me}$ . When  $\Delta T$  reaches  $20^\circ C$ , almost  $q_{nc}$  and  $q_{me}$  can be neglected.

The calculation of the quantities,  $q_{tot}$ ,  $q_b$  and  $A$  in the above equation will be presented in the following part.

$A$  is obtained by Ha (2000). The correlation is expressed as:

$$A = \pi d_{av}^2 \tag{17}$$

where,  $d_{av}$  is time-averaged bubble diameter and represents the diameter of bubbles for coexisting bubbles of all ages. Han and Griffith (1965) assumed that the bubble diameter varies with time as  $t^{1/2}$ , i.e.,

$$d_{av} = \frac{2}{3} D_b \tag{18}$$

where,  $D_b$  is the bubble diameter at departure which was derived by Han and Griffith as:

$$D_b = C_2 \left( \frac{\sigma}{g(\rho_f - \rho_g)} \right)^{1/2} Ja^{*3/4} \tag{19}$$

with  $C_2 = 1.5 \times 10^{-4}$  for water and  $C_2 = 4.65 \times 10^{-4}$  for other liquids. Assuming that if there is no generation of dry spots on the heating surface, heat flux will increase along the extension of nucleate boiling and that each bubble site

has uniform heat duty,  $q_b$  can be evaluated from the following equation:

$$q_b = \frac{h \Delta T_s}{N_a} \tag{20}$$

where  $h$  is heat transfer coefficient which was proposed by Kocamustafaogullari and Ishii as:

$$h = 14.0(k_f N_a^{0.5}) \left[ \frac{(\rho_f C_{pf} \Delta T_s)}{\rho_g h_{fg}} \right]^{0.5} Pr_f^{0.39} N_0^{-0.125} \tag{21}$$

For the pool boiling  $T_g - T_s \cong \Delta T_s$  is used. Where  $N_0$  is the dimensionless nucleation site density which was defined by Kocamustafaogullari and Ishii as:

$$N_0 = N_a D_b^2 \tag{22}$$

**The comparison in pool boiling:**

**CHF calculating procedures:** The basic CHF calculation procedures using Eq. (14)-(16) in pool boiling. Since the correlations for active site density and heat transfer coefficient are given as a function of wall superheat explicitly, the boiling curve showing the dependence of the heat flux on the wall superheat is plotted by substituting Eq. (11), (17) and (20) into (14)-(16). The maximum value of heat flux is taken as the predicted CHF. The procedures for calculating CHF, based on the present fractal model, are summarized as follows:

- Given  $T_\infty$ ,  $T_s$ ,  $T_w$  and  $\phi$ , find the physical properties of the fluid,  $\rho$ ,  $C_{pf}$ ,  $h_{fg}$ ,  $\sigma$ ,  $k_f$ ,  $Pr_f$  and compute  $C_1$  and  $C_3$  in Eq. (8).
- Calculate  $Ja^*$  and  $D_b$  and find  $d_{av}$  from Eq. (18),  $A$  from Eq. (17),  $d_f$  from Eq. (12),  $N_a$  from Eq. (11). 3) Compute the value of  $q_b$  from Eq. (20) and  $q_{tot}$  from Eq. (14)-(16).

**CHF CALCULATING RESULTS AND DISCUSSION**

Dhir and Liaw conducted experiments on the pool boiling of saturated water at 1 atm on a vertical rectangular copper surface with several contact angles. In Fig. 3, the predicted CHF are compared with the data obtained on several partially wetted surfaces. We now compare the results obtained from the above procedures with the experimental results by Dhir and Liaw. Their high heat flux data for contact angles of  $\phi = 14^\circ$ ,  $\phi = 38^\circ$  and  $\phi = 69^\circ$  are presented in Fig. 3a-c, respectively. The solid line in Fig. 3(a)-(c) represent the predictions of CHF versus wall superheat according to the present fractal model, with the value of  $d_f$  computed from Eq. (12) for  $\phi = 14^\circ$ ,  $\phi = 38^\circ$  and  $\phi = 69^\circ$ , respectively. The results shown that the high heat flux from the present fractal

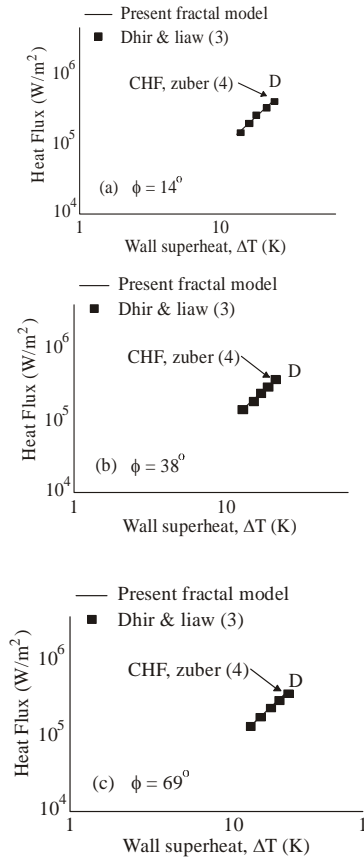


Fig. 3: Comparison of the model predictions and experimental data for several contact angel

model is in excellent agreement with Dhir and Liaw data. The highest point of the boiling curve is CHF point in Fig. 3a-c which is point D in Fig. 1. The predicted CHF is found to be in good agreement with Zuber’s model. As shown in Fig. 3, the surface wettability plays no significant role in the present model. The surface wettability plays no significant role in Zuber’s model for large contact angels more than 27°. As we know, the active nucleation density and bubble departure diameter are affected by contact angel. And the present model shows clearly the mechanism how the contact angel influences CHF.

- Ha obtained  $N_a$  from the pool boiling correlation developed by (Kocamustafaogullari and Ishii, 1983). The correlation is expressed as:

$$N_0 = f(\rho_0)R_0^{-4.4} \quad (23)$$

where,  $N_0$  is the dimensionless nucleation site density,  $R_0$  is the dimensionless cavity size,  $f(\rho_0)$  is the pressure function which are define as:

$$N_0 = N_a D_b^2 \quad (24)$$

$$R_0 = 2R_1/D_b \quad (25)$$

$$f(\rho_0) = 2.157 \times 10^{-7} \rho_0^{-3.2} (1 + 0.0049\rho_0)^{4.13} \quad (26)$$

where,  $\rho_0 = (\rho_f - \rho_g)/\rho_g$ ,  $R_1$  is the cavity radius and  $D_b$  is the bubble departure diameter which is expressed as:

$$D_b = 0.0012\rho_0^{0.9}d_f \quad (27)$$

$$R_1 = \frac{2\sigma}{P_f} \left(1 + \frac{\rho_g}{\rho_f}\right) \left[\exp\left(\frac{h_{fg}(T_g - T_s)}{R_g T_g T_s}\right) - 1\right]^{-1} \quad (28)$$

In Eq. (27),  $d_f$  is the bubble departure diameter of Fritz which is given as:

$$d_f = 0.0208\phi \left[\frac{\sigma}{g(\rho_f - \rho_g)}\right]^{1/2} \quad (29)$$

Ha obtained  $N_a$  from Eq. (23)-(29). But the above expressions are too trivial.

- Ha obtained  $N_a$  from the pool boiling correlation developed by Wang and Dhir (1993). They correlated their data for active nucleation site density as a function of the wall superheat and contact angel as follows:

$$N_a = 5 \times 10^{-27} (1 - \cos\phi) / d_c^6 \quad (30)$$

where,  $d_c$  is the cavity mouth diameter which is a function of the local superheating:

$$d_c = \frac{4\sigma T_s}{\rho_g h_{fg} \Delta T} \quad (31)$$

Eq. (31) did not include the dynamic relation when boiling superheat varies. But the wall temperature and heat flux are very high at heat flux approaching CHF. So Eq. (31) has disadvantage. This paper covers the shortages. The fractal model solves the problem for  $N_a$  of Eq. (14)-(16) successfully. And the expression of active nucleation site applies to CHF, which is predicted in the proposed model quantitatively. An excellent agreement between the proposed mode predictions and experimental data is found.

### CONCLUDING REMARKS

A fractal model for CHF is derived based on the fractal distribution of active nucleation site on boiling surfaces. The predicted CHF based on the proposed fractal model is shown in excellent agreement with experimental data. The validity of the present fractal model is thus verified.

The present model shows clearly the mechanism how the contact angel influences CHF and the surface wettability plays no significant role. The proposed model is a function of area (size) fractal dimensional of active nucleation site, maximum and minimum active cavity, wall superheat, the contact angel and physical properties of the fluid with empirical constant  $C_2 = 1.5 \times 10^{-4}$  which is associated with Eq. (19). No additional empirical constants are introduced, this fractal model contains less empirical constants than the conventional correlation equations except for  $C_2 = 1.5 \times 10^{-4}$ . The proposed model solves the problem for  $N_a$  of Eq. (14)-(16) successfully. The expression of active nucleation site applies to CHF, which is predicted in the proposed model quantitatively. The predicted CHF is shown in excellent agreement with experiment data. The researchers applied empirical formula of bubble departure diameter for the calculation of nucleate boiling heat transfer ago. Therefore, it is uncertain whether these analytical models are reliable. Inertia force of the fluid around the bubbles isn't considered for calculation  $D_b$ , which isn't appropriate. The proposed model applies analytical expressions of bubble departure diameter to compute CHF. And it is a difficulty which all researchers face. The empirical constant  $C_2$  may be eliminated from the proposed model if an analytical expression can be obtained for the bubble departure diameter based on the fractal characteristics of cavities. It will be another aspect of our future study.

### NOMENCLATURE

A	Area by Eq. (17)
$C_{pf}$	Specific heat at constant pressure
$D_b$	Bubble diameter at departure
$D_c$	Cavity diameter
$D_s$	Spot diameter on surface
$d_{av}$	Time-averaged bubble diameter
$d_f$	Fractal dimension
f	Frequency of bubble departure
g	Gravity acceleration
h	Heat transfer coefficient by Eq. (21)
$h_{fg}$	Latent heat of evaporation
$Ja^*$	Jacob number, $\frac{\rho_f C_{pf} T_s}{\rho_g h_{fg}}$
$k_f$	Thermal conductivity
N	Cumulative number of spots
$q_{CHF}$	Critical heat flux
$R_g$	Ideal gas constant $\frac{J}{kg \cdot K}$

T	Temperature
$\Delta T$	Wall superheat

### Greek symbols

$\rho$	Density
$\phi$	Contact angel
$\sigma$	Surface tension of fluid
$\theta_s = T_s - T_\infty$	
$\theta_w = T_w - T_\infty$	

### Subscripts

b	Boiling
f	Liquid phase
g	Gas phase
$N_a$	Cumulative number of active with diameter greater than or equal to $D_c$
n	Number of active nucleation sites
$P_{ff}$	Prandtl number
q	Heta flux
max	Maximum
min	Minimum
me	Microlayer evaporation
nc	Natural convection
s	Saturation condition
tot	Total
w	Wall

### ACKNOWLEDGMENT

This study was supported by the National Natural Science Foundation of China through grant number 11102100 and the Scientific Research Special Foundation for Provincial University of Education Department of Fujian Province of China through grant number JK2011056.

### REFERENCES

- Addoms, J.N., 1948. Heat transfer at high rates to water boiling outside cylinder. D.Sc. Thesis, Chem. Eng. Department, MIT.
- Del Valle, M.V.H. and D.B.R. Kenning, 1985. Subcooled flow boiling at high heat flux. Int. J. Heat Mass Transfer, 28(10): 1907-1920.
- Dhir, V.K. and S.P. Liaw, 1989. Framework for a united model for nucleate and transition pool boiling. ASME J. Heat Transfer, 111: 739-746.
- Feder, J., 1988. Fractals. Plenum Press, New York.
- Gaertner, R.F., 1963. Distribution of active sites in the nucleate boiling of liquids. Chem. Eng. Prog. S. Ser., 59 (41): 52-61.
- Ha, H.C., 1998. A dry-spot model of critical heat flux in pool and forced convection boiling. Int. J. Heat Mass Transfer, 41(2): 303-311.
- Ha, H.C., 2000. A dry-spot model of critical heat flux applicable to both pool boiling and subcooled forced convection boiling, Int. J. Heat Mass Transfer, 43: 241-250.

- Han, C.Y. and P. Griffith, 1965. The mechanism of heat transfer in nucleate pool boiling-Part I and II. *Int. J. Heat Mass Transfer*, 8: 887-913.
- Hsu, Y.Y., 1962. On the size range of active nucleation cavities on a heating surface. *J. Heat Transfer*, 84: 207-215.
- Kang, S., G. Bartsch, D. Jia and X.J. Che. 1994. Probability model to describe Pool Boiling Phenomena. *Proceedings of the Tenth International Heat Transfer Conference, Brighton, U.K.*, 5: 93-98.
- Kocamustafaogullari G. and M. Ishii, 1983. Interfacial area and nucleation site density in boiling systems. *Int. J. Heat Mass Transfer* 26(9): 1377-1387.
- Kutateladze, S.S., 1951. A hydrodynamic theory of changes in boiling process under free convection, *Izv. Akademia Nauk Otdelime Tekh. Nauk*, 4: 529-536.
- Lorenz, J.J. and B.B. Mikic, 1974. Rohsenow, Effect of surface condition on boiling characteristics, In: *Proceedings of the 5th International Heat Transfer Conf, Tokyo*.
- Majumdar, A. and C.L. Tien, 1987. Fractal characteristics and simulation of rough surface. *Wear*, 136: 313.
- Mandelbrot, B.B., 1982. *The Fractal Geometry of Nature*. W.H. Freeman, New York.
- Majumdar, A.A. and B. Bhushan, 1990. Role of fractal geometry in roughness characterization and contact mechanics of surface. *ASME J. Tribol.*, 112: 205-216.
- Majumdar, A., 1992. Role of fractal geometry in the study of thermal phenomena. *Annu. Rev. Heat Transfer*, 4: 51-110.
- Mikic, B.B. and W.M. Rohsenow, 1969. A new correlation of pool boiling data including the effect of surface characteristic, *Trans. ASME. J. Heat Mass Transfer*, 91: 245.
- Sultan, M. and R.L. Judd, 1978. Spatial Distribution of active sites and bubble flux density. *ASME J. Heat Transfer*, 100: 56-62.
- Wang, C.H. and V.K. Dhir, 1993. Effect of surface wettability on active nucleation site density during pool boiling of water on a vertical surface. *ASME J. Heat Transfer*, 115: 659-669.
- Yu, B.M. and P. Cheng, 2002a. Fractal models for the effective thermal conductivity of bidispersed porous media, *AIAA J. Thermophysics Heat Transfer*, 16 (1): 22-29.
- Yu, B.M. and P. Cheng, 2002b. A fractal model for nucleate pool boiling heat transfer. *ASME J. Heat Transfer*, 124: 1117-1124.
- Zuber, N. and J.W. Westwater, 1961. *The Hydrodynamic Crisis in Pool Boiling of Saturated and Subcooled Liquids*. 2nd International Heat Trans. Conference Paper 27, Denver.
- Zuber, N., M. Tribus and J.W. Westwater, 1962. Hydrodynamic crisis in pool boiling of saturated and subcooled Liquids, author' reply. *International Heat Transfer Conference Discussion*, pp: D-84-D-94.